Contents list available at IJRED website

International Journal of Renewable Energy Development

Journal homepage: https://ijred.undip.ac.id

Effects of Injection Strategies on Mixture Formation and Combustion in a Spark-Ignition Engine Fueled with Syngas-Biogas-Hydrogen

Thanh Xuan Nguyen-Thi[*1] and Thi Minh Tu Bui[2]

[1]*Faculty of Chemical Engineering, University of Science and Technology-The University of Danang, Danang, Vietnam*

[2]*Faculty of Electronics & Telecommunication Engineering, University of Science and Technology-The University of Danang, Danang, Vietnam*

Abstract. The paper presents the effects of blend injection and dual injection strategies on mixture formation and combustion of syngas-biogas-hydrogen fueling engine working in the solar-biomass hybrid renewable energy system. The research was performed by simulation method on a retrofitted Honda GX200 spark-ignition engine. The results show that at the end of the compression process, in the case of blend injection of 50% syngas-50% biogas, the fuel-rich zone was positioned on the top of the combustion chamber, whereas in the case of dual injection, this zone was found on the top of the piston. In the case of 50% syngas-50% hydrogen supplied, at the end of the compression process, the fuel-rich area observed on the top of the piston with slightly deflected towards the inlet port in both cases of blend and dual injection. When shifting from blend injection mode to dual injection mode, in the case of 50% syngas-50% biogas fueling engine, the mean temperature of the exhaust gas decreased from 1208 K to 1161 K and the NO_x concentration decreased from 1919 ppm to 1288 ppm. In the case of a 50% syngas-50% hydrogen fueling engine, the mean exhaust gas temperature decreases from 1283 K to 1187 K leading to a decrease in NO_x concentration from 3268 ppm to 2231 ppm. The dual injection has the advantage of lower NO_x emission, whereas the blend injection has the advantage of higher efficiency.

Keywords: Hybrid renewable energy system, Biogas, Syngas, Hydrogen, Gaseous SI engine

1. Introduction

With the aim of limiting the increase in atmospheric temperature below 2°C compared to the pre-industrial levels under the commitment of the 2015 Paris Agreement, the annual global CO_2 emission ought to be reduced to Zero or Net Negative by the middle of the 21st Century (Bakır *et al.*, 2022; Malla *et al.*, 2022; Masson-Delmotte *et al.*, 2018). As reported, internal combustion engine-based transportation means are found to be the main source of emitting toxic emissions including NOx, CO, HC, PM, and soot into the environment, which could be clearly seen during the lockdown period in Covid19 pandemic (Al-Tawaha *et al.*, 2019; Balasubramanian *et al.*, 2020; Huynh *et al.*, 2021; Ölçer *et al.*, 2020), resulting in the environmental pollution and climate change (Atarod *et al.*, 2020; Sandro *et al.*, 2021; Vinayagam *et al.*, 2021). Therefore, in recent years, there have been a large number of studies focusing on improving the combustion characteristics of internal combustion engine by using biofuels such as bioethanol, butanol, biodiesel, bio-oil, furan-based biofuel, ether, ammoniac, and others (Le *et al.*, 2021; Nguyen *et al.*, 2020; Hoang and Pham, 2021; Tabatabaei *et al.*, 2021; Tran *et al.*, 2022; Veza *et al.*, 2022b, 2022c, 2021); using additives/nano-additives/bio-additives (Ağbulut *et al.*, 2022; Hoang, 2021; Lawrence *et al.*, 2022; Nachippan *et al.*, 2022; S. K. Nayak *et al.*, 2021; Rajamohan *et al.*, 2022; Vali *et al.*, 2022), transferring internal combustion engine to the electric/hybrid propulsion (Bui *et al.*, 2021b; Pham

and Hoang, 2019; H. P. Nguyen *et al.*, 2020, 2021; Subramanian *et al.*, 2021), application of advanced injection strategies (Hoang, 2020a; Khandal *et al.,* 2017), or application of low-temperature combustion mode *(*Elumalai *et al.,* 2022; Ganesan *et al.,* 2022) aiming to minimize the above-mentioned toxic emissions. Indeed, developing a strategy to achieve the goal of Net Zero emissions is becoming more and more imperative for countries around the world (Escalante *et al.*, 2022; Lee *et al.*, 2022; X. P. Nguyen *et al.*, 2021a; Rogelj *et al.*, 2021; Said *et al.*, 2022; Sharma *et al.*, 2022c, 2022b).

As reported in the literature, using renewable energy is considered a sagacious approach to attain a Net Zero strategy (Chen *et al.*, 2021a; Foley *et al.*, 2022; Vakili *et al.*, 2022), in which solar, wind, tidal, hydropower, biomass are known as available and cheap renewable energy sources (Chen *et al.*, 2021b; Nižetić *et al.*, 2021; Pandey *et al.*, 2022; Wang *et al.,* 2022). Moreover, to reach net zero emissions, countries need to stop applying coal projects and developing renewable power plants. Indeed, Vietnam is a tropical country where solar power, wind power, and biomass are abundant (Huang *et al.*, 2022; X. P. Nguyen *et al.*, 2021b). However, the main disadvantage of renewable energy power plants is unstable, the generation capacity randomly changes according to climate and weather conditions. Therefore, to ensure the stability of the renewable energy system, it is necessary to coordinate the use of different renewable energy sources, called hybrid renewable energy systems (HRES) (Chandrasekaran *et al.*, 2021; Xuan *et al.*, 2021).

[*] Corresponding author
Email: nttxuan@dut.udn.vn (T.X. Nguyen-Thi)

T.X. Nguyen-Thi and T.M.T. Bui

Int. J. Renew. Energy Dev 2023, 12(1), 118-128

| 119

Fig. 1 presents a hybrid renewable energy system that combines solar energy and biomass energy. The working principle of a solar-biomass HRES is as follows: the hard degradable solid wastes in rural areas are processed into fuel pellets RDF and then transformed into syngas through a gasification process while degradable organic wastes are used to produce biogas (Atabani *et al.*, 2022; Forruque *et al.*, 2022; Goldfarb *et al.*, 2022; Petar *et al.*, 2022). When the capacity of solar power is higher than the load capacity, the excess power is used to produce hydrogen through the electrolysis system (Imanuella *et al.*, 2022). Syngas, biogas, and hydrogen are stored together in gaseous fuel storage bags. When the required load is greater than the capacity of the solar system, the generator powered by the gas engine provides supplementary energy (Bui *et al.*, 2022). Due to the random conditions of gas fuel production, the compositions of the biogas-syngas-hydrogen mixture vary in a large range. Therefore, the fuel supply system for the engines working in HRES must also be flexibly adjusted to improve combustion efficiency and reduce pollutant emissions.

The air-to-fuel ratio (V_{air}/V_{fuel}) of syngas is much lower than that of conventional fuels (Rakopoulos and Michos, 2008). This is a huge engineering challenge for the engine's fuel supply system. A low V_{air}/V_{fuel} value leads to prolonging injection time, which means that the fuel supplied to a cycle is not fully drawn into the cylinder at the end of the intake stroke. This makes it impossible for the engine's equivalence ratio to reach the stoichiometric value, especially for high-speed engines. On the other hand, fuel accumulated on the intake manifold during the previous cycle makes losing control of the mixture equivalence ratio in subsequent cycles and creates the backfire phenomenon. Therefore, with a low V_{air}/V_{fuel} ratio of fuel, the mixing device must not only be able to create a homogeneous fuel-air mixture but also ensure that all fuel supplied to the cycle is sucked into the cylinder at the end of the intake stroke.

In the syngas-biogas-hydrogen fuel, the hydrogen component plays a significant role in mixture formation and combustion. The problems related to hydrogen need to be concerned such as early combustion, backfire high combustion temperature, high-pressure rise, and increase in NO_x concentration (Heffel, 2003; Hoang and Pham, 2020; Ma *et al.*,

2007). Many studies on fuel supply systems for spark-ignition (SI) engines using gaseous fuels have been reported about the addition of a hydrogen injector on the intake manifold to improve the performance of the gasoline SI engine (Banapurmath *et al.*, 2011; Fiore *et al.*, 2020; Ji and Wang, 2011; Konde and Yarasu, 2014; Le *et al.*, 2020). Adjusting injection time to reduce the amount of hydrogen residual on the intake manifold can limit the backfire (Duan *et al.*, 2014; Liu *et al.*, 2008; Subramanian and Salvi, 2016). For SI engines, directly injecting hydrogen into the combustion chamber improves engine efficiency and reduces pollutant emissions (Fiore *et al.*, 2020; Hagos *et al.*, 2016). Apart from adding hydrogen to the lean fuel mixture, many authors have also studied the addition of HHO (a mixture of 2/3 hydrogen and 1/3 oxygen) into lean mixtures to improve combustion (Bui *et al.*, 2021c). Similar to hydrogen, HHO is very flammable, so the backfire effect on the intake manifold needs to be taken care of. Bui et al. (Bui *et al.*, 2021a) have developed a special mixer to handle this problem. The simulation study on biogas-HHO injection was presented in a study by Bui et al. (Bui *et al.*, 2020). The research results allow to establish a suitable biogas-HHO injection scheme.

However, to our best knowledge, the publication found in the literature mostly focused on sizing the HRES (Çetinbaş *et al.*, 2019; Hassane *et al.*, 2022; Oladeji *et al.*, 2021)The research on engines fueled with renewable gaseous fuel engines focussed mainly on a given fuel or a blend with given fuel compositions. In a solar-biomass HRES, the engine is fueled by a flexible blend with a large variety of compositions. The engine can run on syngas, biogas, hydrogen, or a mixture containing two or three of these fuel components. Due to a significant difference in the V_{air}/V_{fuel} ratio of syngas from the other fuels, there is a huge technical challenge in designing the fuel supply system of the engine fueled by syngas-biogas-hydrogen. For bridging the gap, this work focused on the comparative study of blend injection and dual injection of two couples of fuels: syngas-biogas and syngas-hydrogen. Effects of injection configuration on mixture formation and combustion were analyzed by simulation method. The results help to orient future experimental research to develop an appropriate fuel supply system for the engine operating in solar-biomass HRES.
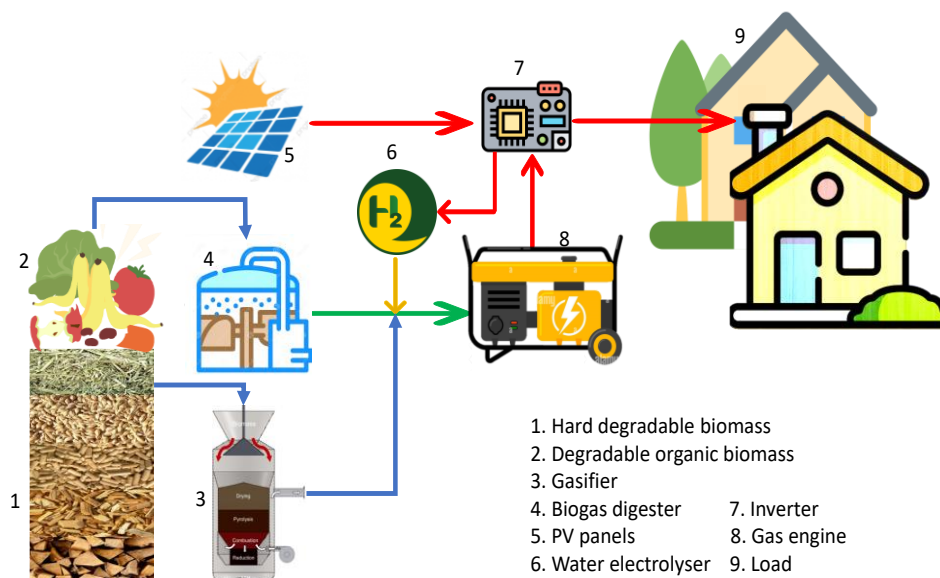

1. Hard degradable biomass
2. Degradable organic biomass
3. Gasifier
4. Biogas digester   7. Inverter
5. PV panels   8. Gas engine
6. Water electrolyser   9. Load

Fig. 1: Diagram of a solar-biomass hybrid renewable energy system

T.X. Nguyen-Thi and T.M.T. Bui

Int. J. Renew. Energy Dev 2023, 12(1), 118-128

| 120

Table 1
Tested fuel compositions

Fuel	Compositions (mol/mol)					M (g/mol)	m_{air}/m_{fuel} (g/g)	V_{air}/V_{fuel} (l/l)
	CH_4	H_2	CO	CO_2	N_2			
Biogas (B)	0.7	0	0	0.3	0	24.40	7.98	6.71
Syngas (S)	0.05	0.18	0.20	0.12	0.45	24.64	1.64	1.39
Hydrogen (H)	0	1	0	0	0	2	34.78	2.4
Blend1 (50S-50H)	0.025	0.59	0.1	0.06	0.225	13.32	4.13	1.9
Blend2 (50S-50B)	0.375	0.09	0.1	0.21	0.225	24.52	4.79	4.05
LHV (MJ/Nm³)	33,906	10,246	12,035	-	-			
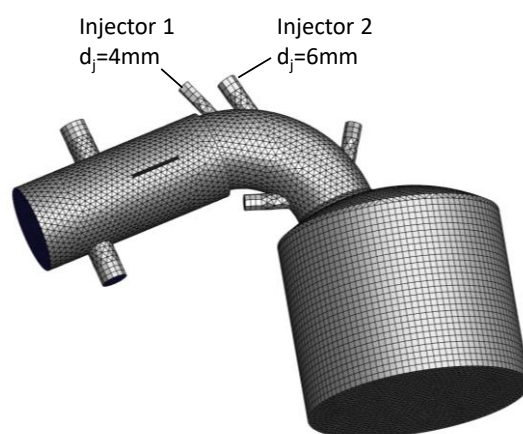
Fig. 2 Computational space meshing and injector positions setting

2. Material and method

2.1 Engine and Fuels

This study was conducted on the syngas-biogas-hydrogen engine converted from the Honda GX200 gasoline engine. The engine has a cylinder diameter of 68mm, piston stroke of 54mm, and compression ratio of 8.5. Originally, it is fueled with gasoline by a traditional carburetor and produced a capacity of 4.8 kW at a speed of 3600 rpm. The main characteristics of biogas, syngas, hydrogen and fuel mixtures used in the study are shown in Table 1.

2.2 Model establishment

The simulation was performed based on Ansys Fluent 2021R1 software. Computational space includes the combustion chamber, cylinder, and intake manifold as shown in Fig. 2. The dynamic meshing was applied for the cylinder volume due to its deformation with crankshaft rotation angle. The system of convection-diffusion equations was closed by the k-ε turbulence model. The thermodynamic parameters of the mixtures were calculated through the Partially Premixed Combustion model. At the entrance of the intake manifold, there is only air, thus the mixture fraction f = 0. The gauge pressure and the temperature of the air at the entrance are 0 bar and 310 K, respectively. At the nozzle inlet, there is only fuel, thus f = 1. The gauge pressure and the temperature of fuel at the nozzle inlet are 1 bar and

320 K, respectively. The local equivalence ratio of the mixture could be calculated in terms of fuel composition and oxygen composition, or through the mixture fraction f. Different injection system configurations were studied (Fig. 2). In this work, only injector 1 (nozzle diameter d_j=4mm) and injector 2 (nozzle diameter d_j=6mm) were considered. Syngas, biogas, and hydrogen can be injected separately through these different nozzles (case of dual injection) or they can be mixed and then injected through a common nozzle (case of blend injection). The detail of model establishment was presented by (Bui *et al.*, 2022).

3. Results and discussion

3.1 Comparison between blend injection and dual injection of syngas-biogas

Fig. 3a shows the contour lines of CH_4, CO, and HC concentration, as well as the equivalence ratio at the positions of 20°CA, 200°CA, and 330°CA, respectively, in the case of blend injection of the Blend2 (50% syngas-50% biogas) through the injectors 1 and 2. The engine operates at a speed of 3000 rpm. The concentration of CH_4 is mainly present in biogas, and the component CO is mainly present in syngas. The results in Fig. 3a show that during the compression and before the combustion takes place, the distribution of individual components of CH_4 and CO, as well as the distribution of the total fuel composition HC in the cylinder, are similar. The zone of high fuel concentration is concentrated towards the cylinder

T.X. Nguyen-Thi and T.M.T. Bui

Int. J. Renew. Energy Dev 2023, 12(1), 118-128

| 121

wall opposite the inlet port. At the end of the compression process, the local equivalence ratio in the combustion chamber varies from 0.9 to 1.12 with a fuel-rich zone located on the top of the combustion chamber.

Fig. 3b shows the variation of the mass flow rate of air (Q_{air}), the mass flow rate of fuel (Q_{fuel}), and the biogas/syngas ratio according to the crankshaft angle φ when the engine was fueled with syngas at speed of n = 3000 rpm. When fuel injection is started at 10°CA, the locally increased pressure pushes some air out of the intake manifold, thus, negative intake airflow is observed. But soon later the airflow increases due to the vacuum in the cylinder created by the piston going down. The biogas/syngas ratio is at a stable value of 100%. Fig. 3c shows that when the blend is introduced into the cylinder, the oxygen concentration decreases, thus the equivalence ratio increases very strongly to the maximum value of φ =2.02 and then gradually decreases to a stable value.

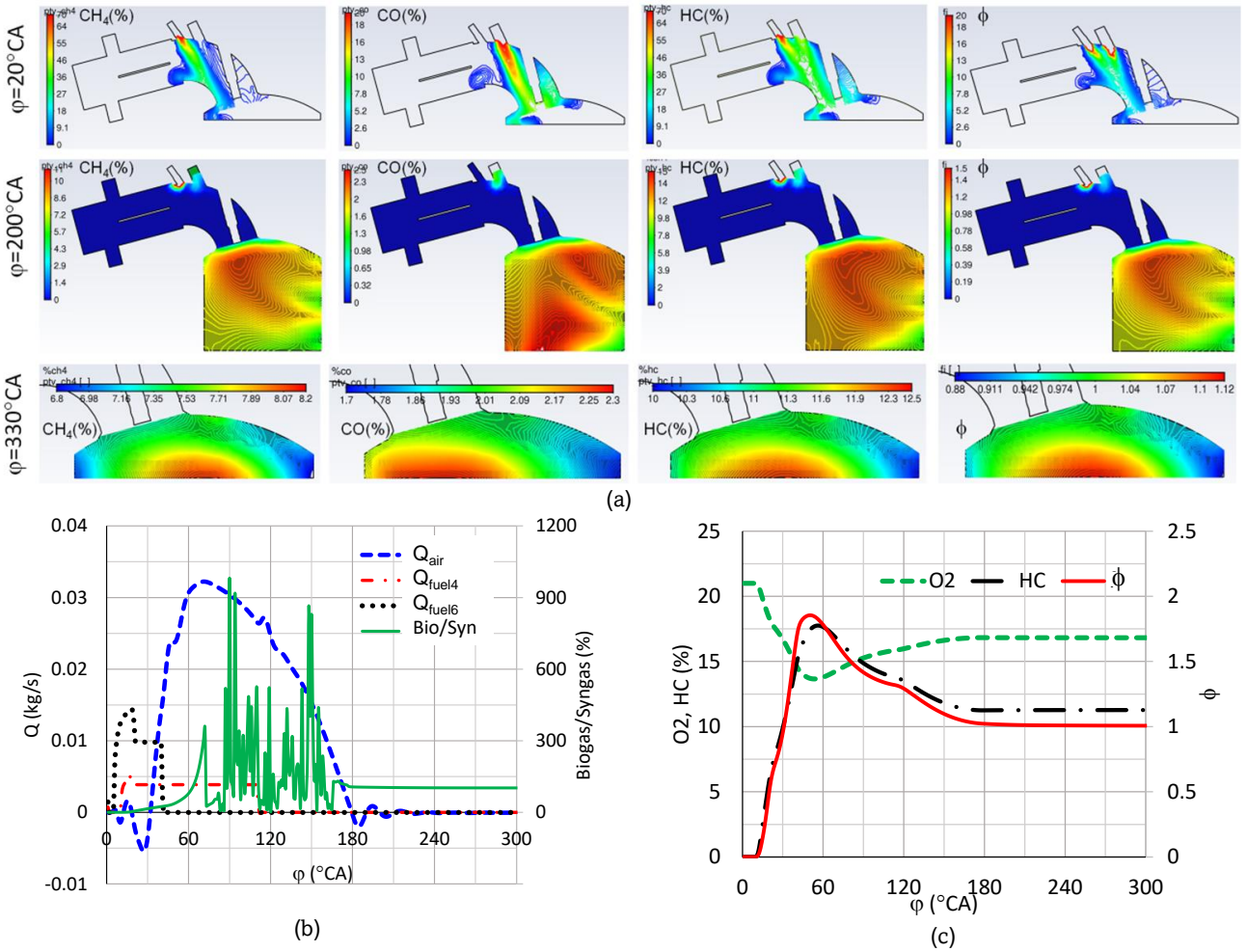Fig. 4a shows the contour lines of CH_4, CO, and HC concentration, as well as the equivalence ratio φ at 20°CA, 200°CA, and 330°CA, respectively, in case of dual injection of syngas and biogas. Syngas is injected through the injector of 6mm nozzle diameter with an injection duration of 36°CA. Biogas is injected through the injector of 4mm nozzle diameter with an injection duration of 100°CA. Unlike the case of blend

injection, in the case of dual injection, CH_4 (representing biogas) and CO (representing syngas) are distributed differently in the cylinder. The rich CH_4 content zone is concentrated near the inlet port, while the high CO concentration zone is composed of two areas, one area on the top of the piston and the other moving towards the exhaust port. At the end of the compression stroke, the high CH_4 zone is concentrated in the center of the piston top, and the CO-rich area is located on the piston half towards the inlet port.

As can be seen from the chart of Fig. 4b, the curve of the biogas/syngas ratio fluctuates strongly during the intake process in the case of dual injection. This is because biogas and syngas are injected into the intake manifold through two separate nozzles, so they do not enter the cylinder at the same time. The biogas/syngas ratio is high when the syngas composition is low, producing peaks. In the case of blend injection, the mixture of syngas and biogas goes into the cylinder at the same time, so the ratio of biogas/syngas is determined from the beginning. The curve of the biogas/syngas ratio reached a stable value of 100%, equivalent to the Blend2 fuel mixture (50% syngas and 50% biogas), during the compression process. Along with this injection condition, the equivalence ratio of the mixture reaches a stoichiometric value (Fig. 4c).
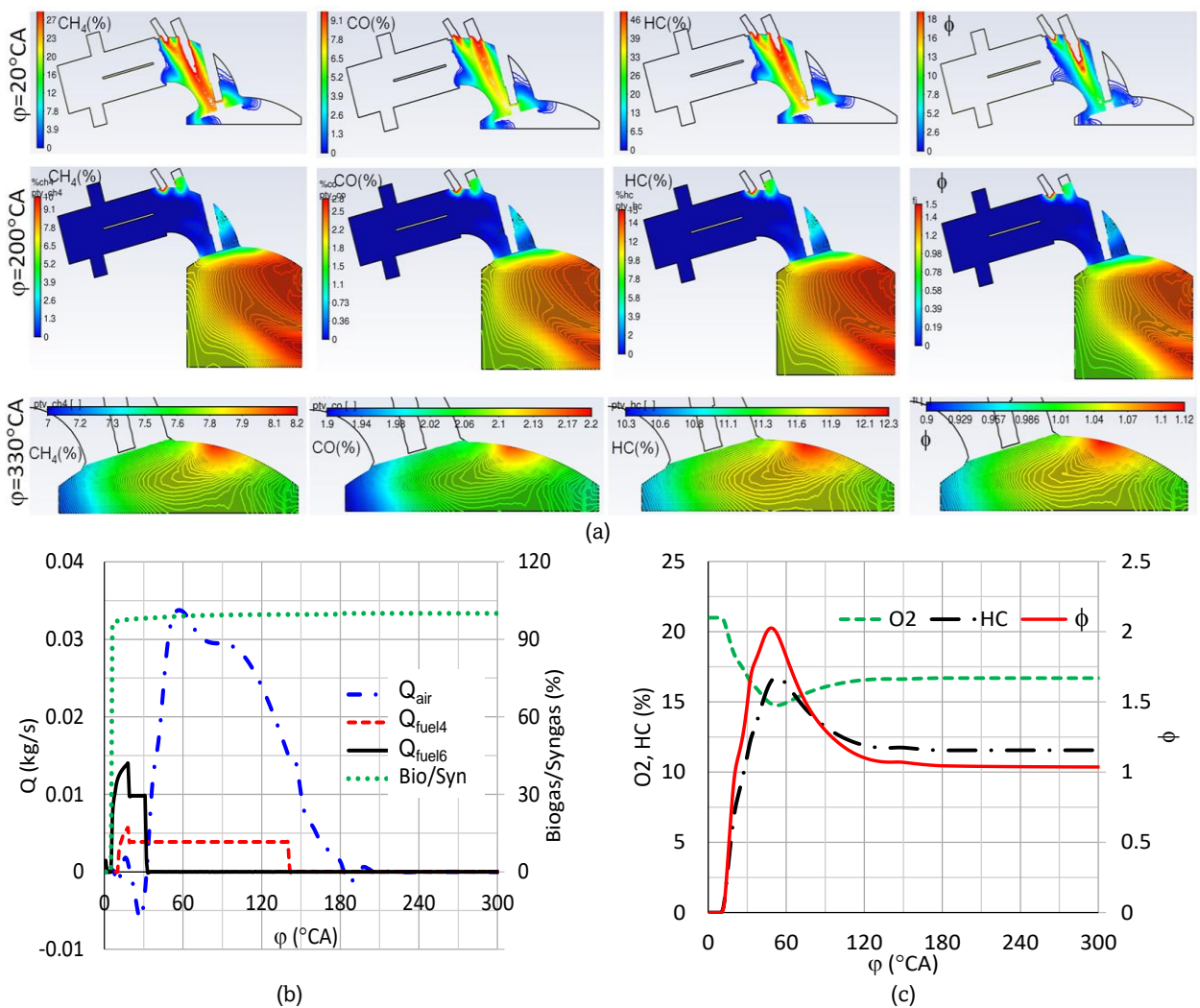
Fig. 3 Mixture formation when injecting the Blend2 through injector 1 and injector 2: (a). Contour lines of CH_4, CO, HC concentration, and f at 20°CA, 200°CA, and 330°CA, respectively; (b). Variation of the mass flow rate of air, fuel, and biogas/syngas ratio with crankshaft angle; (c). Variation of O_2, HC concentrations, and φ with crankshaft angle

T.X. Nguyen-Thi and T.M.T. Bui

Int. J. Renew. Energy Dev 2023, 12(1), 118-128

| 122

(a)

(b)

(c)

Fig. 4 Mixture formation with the dual injection of biogas through injector 1 and syngas through injector 2: (a). Contour lines of CH_4, CO, HC concentration, and f at 20°CA, 200°CA, and 330°CA, respectively; (b). Variation of the mass flow rate of air, fuel, and biogas/syngas ratio with crankshaft angle; (c). Variation of O_2, HC concentrations, and ϕ with crankshaft angle

(a) Blend injection
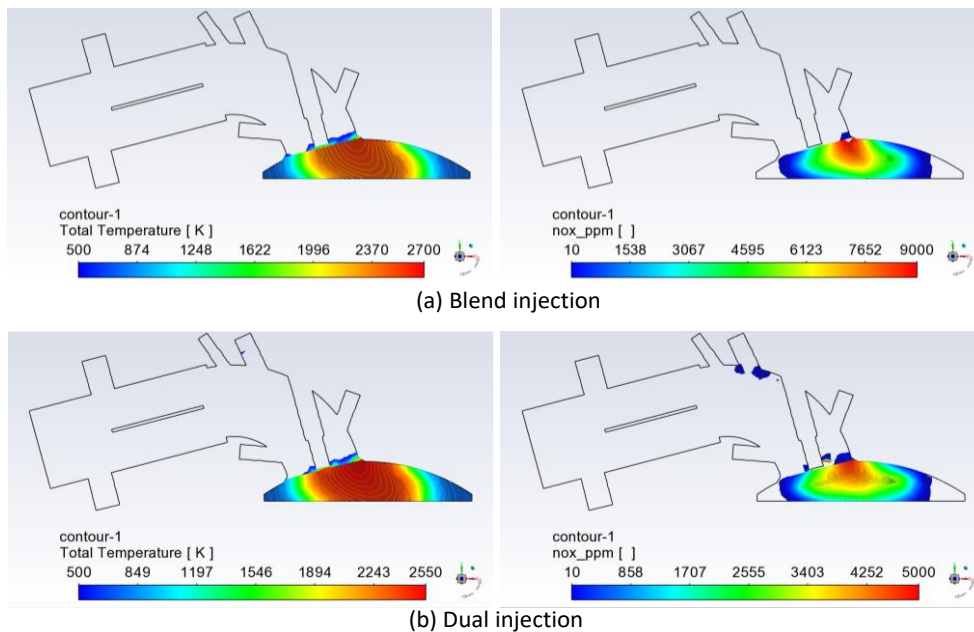
(b) Dual injection

Fig. 5 Contours lines of temperature and NO_x concentration at 370°CA in the case of blend injection (a) and dual injection (b) with syngas-biogas through the injector 1 and the injector 2 (50% syngas, 50% biogas, n=3000rpm)

T.X. Nguyen-Thi and T.M.T. Bui

Int. J. Renew. Energy Dev 2023, 12(1), 118-128

| 123

Fig. 5a and Fig. 5b compare the temperature contours and the NO$_x$ concentration contours on the axisymmetric plan of the combustion chamber at 35°CA after ignition in the case of blend injection and dual injection of the Blend2. It can be seen that the zone of high combustion temperature is located around the area of ϕ approximately 1. As shown in Fig. 3a and Fig. 4a, the mixture in the combustion chamber right at the moment of ignition in the case of dual injection is less homogeneous than that in the case of blend injection, therefore the average combustion temperature of the first case is lower than that of the second case (Veza *et al.*, 2022a). Due to the NO$_x$ formation being strongly affected by the temperature, the zone of high NOx concentration is found in the same region of high temperature (Aykut *et al.*, 2021; Cao *et al.*, 2020; Hoang, 2020b). In the case of dual injection, the flame front tends to move towards the zone of the rich mixture. The maximum combustion temperature in the case of dual injection is lower than that in the case of blend injection, hence the maximum concentration of NO$_x$ in the case of dual injection is also lower than that of blend injection (B. Nayak *et al.*, 2021; Sharma *et al.*, 2022a).

Fig. 6. compares the variation of pressure (Fig. 6a), and, temperature (Fig. 6b), and NO$_x$ concentration (Fig. 6c) according to crankshaft angle in the case of blend injection with the Blend2 and dual injection with 50% syngas and 50% biogas. As seen from these figures, the in-cylinder pressure slightly decreases when shifting from blend injection mode to dual injection mode, resulting in a decrease in indicative engine work cycle from 175 J/cyc to 168 J/cyc, i.e. a reduction of engine power of 4%. The mean exhaust gas temperature decreased from 1208 K to 1161 K when switching from blend injection to dual injection (Fig. 6b). The NO$_x$ concentration in the exhaust gas decreased from 1919 ppm to 1288 ppm when switching from the blend injection mode to dual injection mode (Fig. 6c), corresponding with the reduction of temperature in these two cases.

### 3.2 Comparison between blend injection and dual injection of syngas-hydrogen

Identical to the case of syngas-biogas injection, in the case of syngas-hydrogen blend injection, there is no significant difference in the distribution of CO and H$_2$ concentrations in the cylinder. At the end of the compression process, the fuel-rich area located on the top of the piston is slightly deflected towards the inlet port (Fig. 7a). The curve of the H$_2$/syngas ratio is stable when the fuel mixture enters the cylinders because the fuels were mixed (Fig. 7b). With the injection duration of 130°CA through an injector of 4mm nozzle diameter and 46°CA through the injector of 6mm nozzle diameter, the stoichiometric air-fuel mixture was obtained (Fig. 7c).

Fig. 8a shows the contour lines of H$_2$, CO, and HC in the case of dual injection. Hydrogen was injected through the injector of a 4mm nozzle diameter and syngas was injected through a 6mm nozzle diameter. During the compression stroke, the distribution of hydrogen completely deviated from the cylinder wall towards the inlet port. This skewed distribution takes place towards the end of the compression. At the end of the compression process, the hydrogen concentration in the combustion chamber varies from a minimum of 19% to a maximum of 24% (Fig. 8a). Meanwhile, in the case of blend injection, the hydrogen concentration in the combustion chamber varies from 18% to 22% (Fig. 7a). Therefore, it can be concluded that in the case of syngas-hydrogen mixture

supplied, the blend or dual-injection method does not affect the distribution of fuel concentration in the combustion chamber. In the case of dual injection, the hydrogen/syngas ratio fluctuates strongly during the intake stroke and then becomes stable during the compression stroke (Fig. 8b). With the injection duration of 77°CA for both injectors, the stoichiometric mixture is obtained (Fig. 8c).
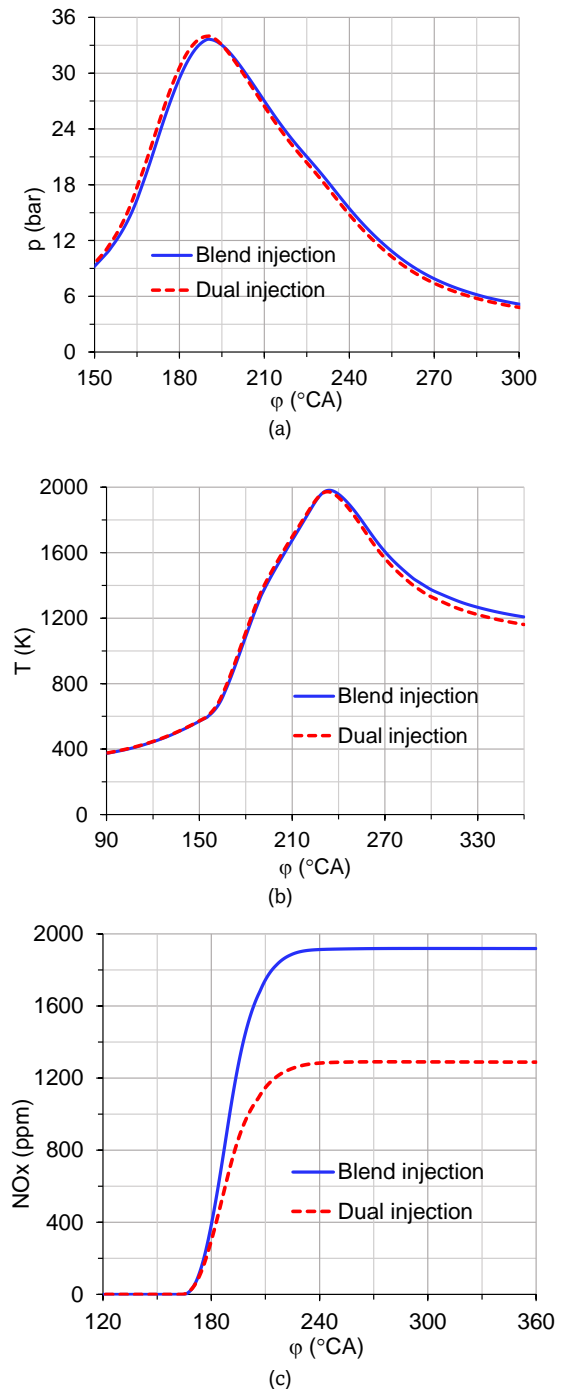

Fig. 6 Variation of pressure (a), temperature (b), and NO$_x$ concentration (c) in case of blend injection and dual injection with syngas-biogas through the injector 1 and the injector 2 (50% syngas, 50% biogas, n=3000rpm)

T.X. Nguyen-Thi and T.M.T. Bui   *Int. J. Renew. Energy Dev 2023, 12(1), 118-128*

| 124
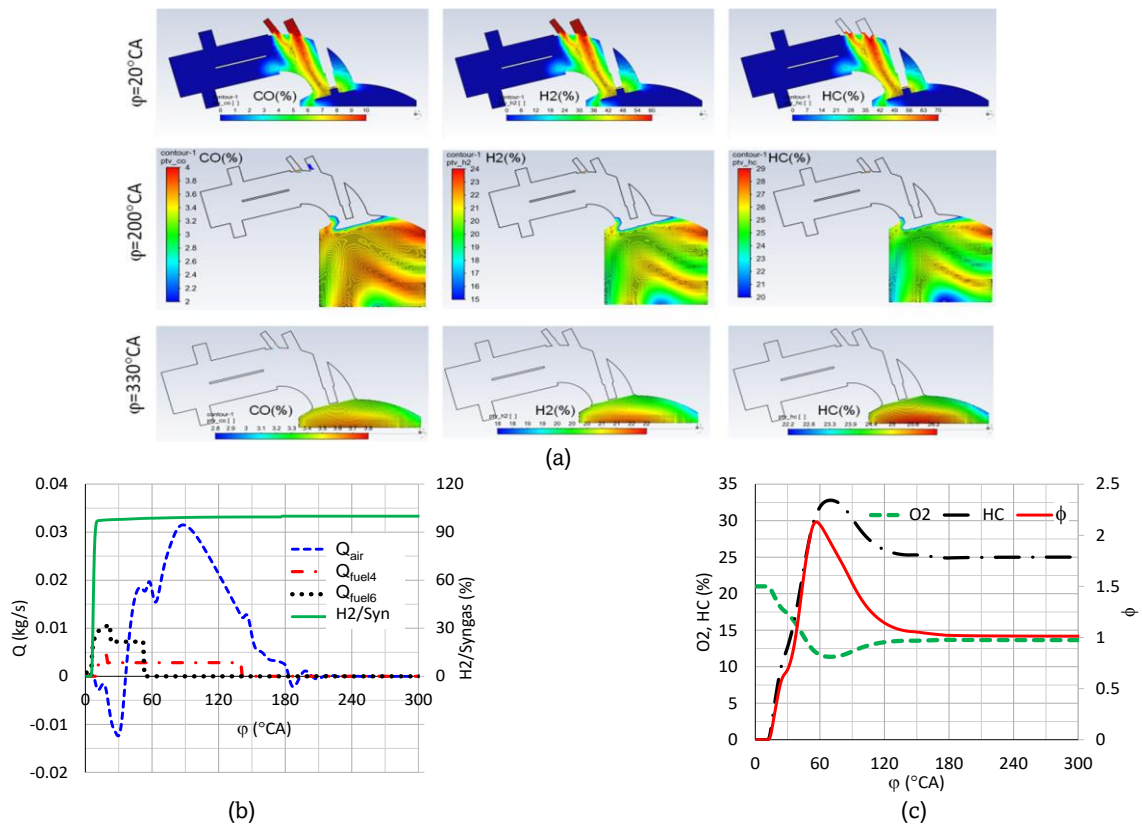
Fig. 7 Mixture formation when injecting the Blend1 through injector 1 and injector 2: (a). Contour lines of CO, H₂, and HC at 20°CA, 200°CA, and 330°CA, respectively; (b). Variation of the mass flow rate of air, fuel, and hydrogen/syngas ratio with crankshaft angle; (c). Variation of O₂, HC concentrations, and ϕ with crankshaft angle
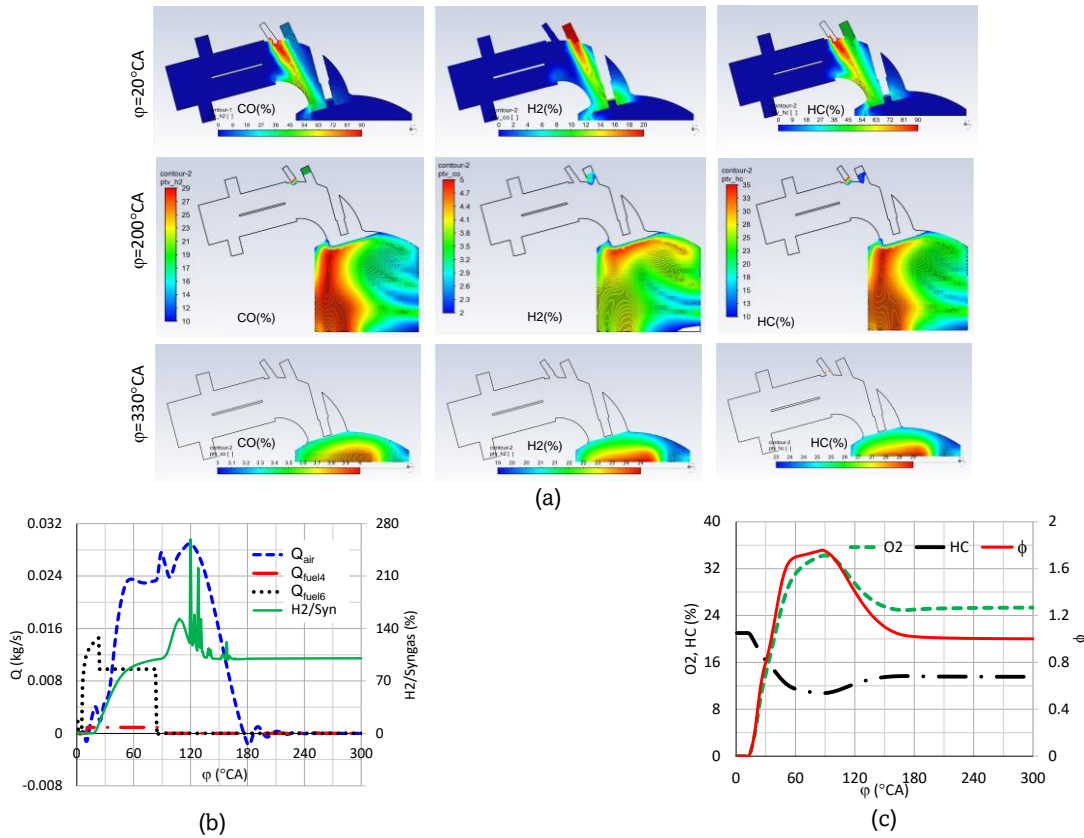
Fig. 8 Mixture formation with a dual injection of hydrogen through injector 1 and syngas through injector 2: (a). Contour lines of CO, H₂, and HC at 20°CA, 200°CA, and 330°CA, respectively; (b). Variation of the mass flow rate of air, fuel, and hydrogen/syngas ratio with crankshaft angle; (c). Variation of O₂, HC concentrations, and ϕ with crankshaft angle

T.X. Nguyen-Thi and T.M.T. Bui

Int. J. Renew. Energy Dev 2023, 12(1), 118-128

| 125
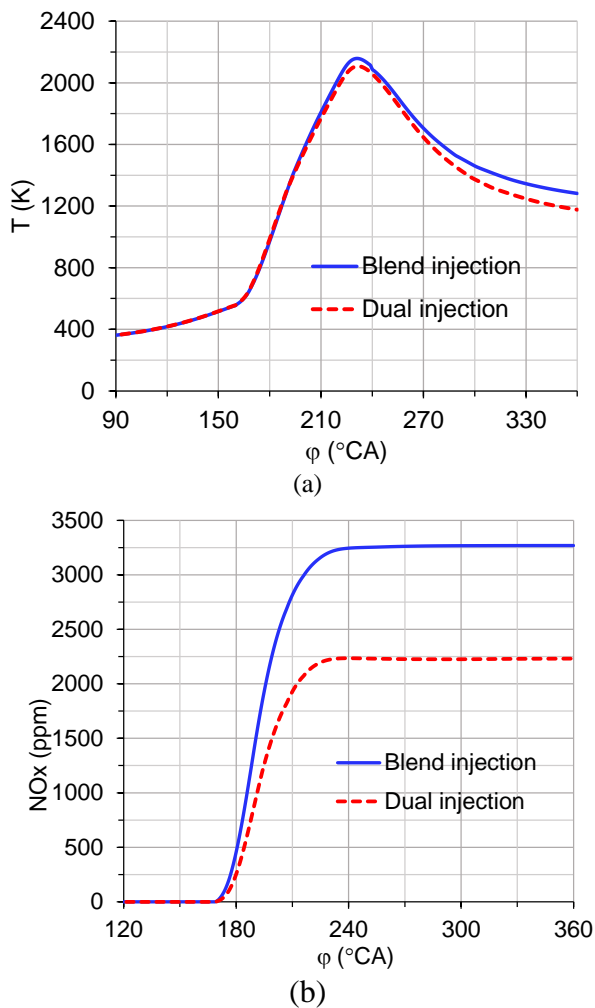
Fig. 9 Variation of temperature (a) and NO$_x$ concentration (b) in case of blend injection and dual injection of syngas-hydrogen through injector 1 and injector 2 (50% syngas, 50% hydrogen, n=3000rpm)

In the same manner as the above case, when shifting from blend injection mode to dual injection mode of the Blend1, the average temperature of the exhaust gas decreases from 1283K to 1187 K (Fig. 9a) leading to a decrease in NO$_x$ concentration from 3268ppm to 2231 ppm (Fig. 9b). The combustion temperature of the syngas-hydrogen mixture is higher than that of the syngas-biogas mixture, so the NO$_x$ content in the exhaust gas of the syngas-hydrogen fueling engine is higher than that on syngas-biogas fueled engine. In both cases, NO$_x$ concentrations were reduced in the case of dual injection compared to blend injection.

4. Conclusion

From the obtained results, it could be concluded that, at the end of the compression process, in the case of blend injection of 50% syngas-50% biogas, the fuel-rich zone is located on the top of the combustion chamber, whereas in the case of dual injection, the fuel-rich zone is positioned on the top of the piston with the equivalence ratio varies in the range from 0.9 to 1.12. In the case of 50% syngas-50% hydrogen fuel supplied, at the end of the compression process, the fuel-rich area concentrated

on the top of the piston with slightly deflected towards the inlet port in both cases of blend and dual injections. The difference in hydrogen concentration in the combustion chamber is less than 5%.

When shifting from blend injection mode to dual injection mode, in the case of a 50% syngas-50% biogas fueled engine, the average temperature of the exhaust gas decreased from 1208 K to 1161 K and the NO$_x$ concentration decreased from 1919 ppm to 1288 ppm with a reduction of 4% in engine power. In the case of a 50% syngas-50% hydrogen fueling engine, the average temperature of the exhaust gas decreases from 1283 K to 1187 K leading to a decrease in NO$_x$ concentration from 3268 ppm to 2231 ppm. The simulation results show that a flexible adjusting fuel supply system is needed for the engine working in a solar-biomass hybrid renewable energy system. The difference in the distribution of fuel concentrations according to dual and blend injection strategies allows an appropriate design of the combustion chamber. The dual injection has the advantage of lower NO$_x$ emission, whereas blend injection has the advantage of higher efficiency. These observations orient the future experimental research of the engine.

Author Contributions: Thanh Xuan Nguyen-Thi: Conceptualization, methodology, resources, writing-original draft, supervision; Thi Minh Tu Bui: Simulation, writing-review, and editing. All authors have read and agreed to the published version of the manuscript.

Conflicts of Interest: The authors declare no conflict of interest.

References

Ağbulut, Ü., Huang, Zuohua, Veza, I., (2022). Understanding behaviors of compression ignition engine running on metal nanoparticle additives-included fuels: A control comparison between biodiesel and diesel fuel. *Fuel* 326, 124981. https://doi.org/10.1016/j.fuel.2022.124981.

Al-Tawaha, A.R.M.S., Pham, V.V., Tran, Q.V., (2019). Comparative analysis on performance and emission characteristics of an in-Vietnam popular 4-stroke motorcycle engine running on biogasoline and mineral gasoline. *Renew. Energy Focus* 28, 47–55. https://doi.org/10.1016/j.ref.2018.11.001.

Atabani, A.E., Mahmoud, E., Aslam, M., Naqvi, S.R., Juchelková, D., Bhatia, S.K., Badruddin, I.A., Khan, T.M., Palacky, P., (2022). Emerging potential of spent coffee ground valorization for fuel pellet production in a biorefinery. *Environ. Dev. Sustain.* 1–39. https://doi.org/10.1007/s10668-022-02361-z.

Atarod, P., Khlaife, E., Aghbashlo, M., Tabatabaei, M., Mobli, H., Nadian, M.H., Hosseinzadeh-Bandbafha, H., Mohammadi, P., Roodbar Shojaei, T., Mahian, O., Gu, H., Peng, W., Lam, S.S., (2021). Soft computing-based modeling and emission control/reduction of a diesel engine fueled with carbon nanoparticle-dosed water/diesel emulsion fuel. *J. Hazard. Mater* 407. 124369. https://doi.org/10.1016/j.jhazmat.2020.124369.

Aykut, Ö.I., Nižetić, S., Tuan, HA., (2021). Prospective review on the application of biofuel 2, 5-dimethylfuran to diesel engine. *Journal of the Energy Institute.* 94, 360–386.

T.X. Nguyen-Thi and T.M.T. Bui   *Int. J. Renew. Energy Dev 2023, 12(1), 118-128*

| 126

https://doi.org/10.1016/j.joei.2020.10.004.

Bakır, H., Ağbulut, Ü., Gürel, A.E., Yıldız, G., Güvenç, U., Soudagar, M.E.M., Deepanraj, B., Saini, G., Afzal, A., (2022). Forecasting of future greenhouse gas emissions trajectory for India using energy and economic indexes with various metaheuristic algorithms. *J. Clean. Prod.* 360, 131946. https://doi.org/10.1016/j.jclepro.2022.131897.

Balasubramanian, D., Konur, O., Bui, T.T., Nguyen, D.C., Tran, V.N., (2020). Characteristics of PM and soot emissions of internal combustion engines running on biomass-derived DMF biofuel: a review. *Energy Sources, Part A Recover. Util. Environ. Eff.* 1–22. https://doi.org/10.1080/15567036.2020.1869868.

Banapurmath, N.R., Yaliwal, V.S., Kambalimath, S., Hunashyal, A.M., Tewari, P.G., (2011). Effect of wood type and carburetor on the performance of producer gas-biodiesel operated dual fuel engines. *Waste and Biomass Valorization* 2, 403–413. https://doi.org/10.1007/s12649-011-9083-5.

Bui, V.G., Bui, T.M.T., Nizetic, S., Nguyen Thi, T.X., Vo, A.V., (2021a). Hydrogen-Enriched Biogas Premixed Charge Combustion and Emissions in DI and IDI Diesel Dual Fueled Engines: A Comparative Study. *J. Energy Resour. Technol.* 143, 1–13. https://doi.org/doi.org/10.1115/1.4051574.

Bui, V.G., Bui, T.M.T., Ong, H.C., Nižetić, S., Nguyen, T.T.X., Atabani, A.E., Štěpanec, L., 2022. Optimizing operation parameters of a spark-ignition engine fueled with biogas-hydrogen blend integrated into biomass-solar hybrid renewable energy system. *Energy* 252, 124052. https://doi.org/10.1016/j.energy.2022.124052.

Bui, V.G., Minh Tu Bui, T., Nižetić, S., Sakthivel, R., Nam Tran, V., Hung Bui, V., Engel, D., Hadiyanto, H., (2021b). Energy storage onboard zero-emission two-wheelers: Challenges and technical solutions. *Sustain. Energy Technol. Assessments* 47, 101435. https://doi.org/10.1016/J.SETA.2021.101435.

Bui, V.G., Tran, V.N., Bui, T.M.T., Vo, A.V., (2020). A simulation study on a port-injection SI engine fueled with hydroxy-enriched biogas. *Energy Sources, Part A Recover. Util. Environ. Eff.* 1–17. https://doi.org/10.1080/15567036.2020.1804487.

Bui, V.G., Vo, T.H., Bui, T.M.T., Nguyen-Thi, T.X., (2021c). Characteristics of Biogas-Hydrogen Engines in a Hybrid Renewable Energy System. *Int. Energy J.* 21, 467–480. http://www.rericjournal.ait.ac.th/index.php/reric/article/view/2785.

Cao, D.N., Luu, H.Q., Bui, V.G., Tran, T.T.H., (2020). Effects of injection pressure on the NOx and PM emission control of diesel engine: A review under the aspect of PCCI combustion condition. *Energy Sources, Part A Recover. Util. Environ. Eff.* 1–18. https://doi.org/10.1080/15567036.2020.1754531.

Çetinbaş, İ., Tamyürek, B., Demirtaş, M., (2019). Design, analysis and optimization of a hybrid microgrid system using HOMER software: Eskisehir osmangazi university example. *Int. J. Renew. Energy Dev.* 8(1), 65-79. https://doi.org/10.14710/ijred.8.1.65-79.

Chandrasekaran, K., Selvaraj, J., Amaladoss, C.R., Veerapan, L., (2021). Hybrid renewable energy based smart grid system for reactive power management and voltage profile enhancement using artificial neural network. *Energy Sources, Part A Recover. Util. Environ. Eff.* 1–24. https://doi.org/10.1080/15567036.2021.1902430.

Chen, W.-H., Chong, C.T., Thomas, S., A.Bandh, S., Ong, H.-C., (2021a). Impacts of COVID-19 pandemic on the global energy system and the shift progress to renewable energy: Opportunities, challenges, and policy implications. *Energy Policy* 154, 112322. https://doi.org/10.1016/j.enpol.2021.112322.

Chen, W.-H., Wang, J.-S., Chang, M.-H., Mutuku, J.K., (2021b). Efficiency improvement of a vertical-axis wind turbine using a deflector optimized by Taguchi approach with modified additive method. *Energy Convers. Manag.* 245, 114609. https://doi.org/10.1016/j.enconman.2021.114609.

Duan, J., Liu, F., Sun, B., (2014). Backfire control and power enhancement of a hydrogen internal combustion engine. *Int. J. Hydrogen Energy* 39, 4581–4589. https://doi.org/10.1016/j.ijhydene.2013.12.175.

Elumalai, P. V, Dash, S.K., Parthasarathy, M., Dhineshbabu, N.R.,

Balasubramanian, D., (2022). Combustion and emission behaviors of dual-fuel premixed charge compression ignition engine powered with n-pentanol and blend of diesel/waste tire oil included nanoparticles. *Fuel* 324, 124603. https://doi.org/10.1016/j.fuel.2022.124603.

Escalante, J., Chen, W.-H., Tabatabaei, M., Kwon, E.E., Lin, K.-Y.A., Saravanakumar, A., (2022). Pyrolysis of lignocellulosic, algal, plastic, and other biomass wastes for biofuel production and circular bioeconomy: A review of thermogravimetric analysis (TGA) approach. *Renew. Sustain. Energy Rev.* 169, 112914. https://doi.org/10.1016/j.rser.2022.112914.

Fiore, M., Magi, V., Viggiano, A., (2020). Internal combustion engines powered by syngas: A review. *Appl. Energy* 276, 115415. https://doi.org/10.1016/j.apenergy.2020.115415.

Foley, A.M., Nižetić, S., Huang, Z., Ong, H.C., Ölçer, A.I., (2022). Energy-related approach for reduction of CO_2 emissions: A critical strategy on the port-to-ship pathway. *J. Clean. Prod.* 355, 131772. https://doi.org/10.1016/j.jclepro.2022.131772.

Forruque, A.S., Said, Z., Rafa, N., Ağbulut, Ü., Veza, I., Huang, Z., Chen, W.-H., (2022). Hydrothermal carbonization of food waste as sustainable energy conversion path. *Bioresour. Technol.* 363, 127958. https://doi.org/10.1016/j.biortech.2022.127958.

Ganesan, N., Ekambaram, P., Balasubramanian, D., (2022). Experimental assessment on performance and combustion behaviors of reactivity-controlled compression ignition engine operated by n-pentanol and cottonseed biodiesel. *J. Clean. Prod.* 330, 129781. https://doi.org/10.1016/j.jclepro.2021.129781.

Goldfarb, J.L., Foley, A.M., Lichtfouse, E., Kumar, M., Xiao, L., Ahmed, S.F., Said, Z., Luque, R., (2022). Production of biochar from crop residues and its application for anaerobic digestion. *Bioresour. Technol.* 363, 127970. https://doi.org/10.1016/j.biortech.2022.127970.

Hagos, F.Y., Aziz, A.R.A., Sulaiman, S.A., Mahgoub, B.K.M., (2016). Low and Medium Calorific Value Gasification Gas Combustion in IC Engines, in: Developments in Combustion Technology. *InTech.* https://doi.org/10.5772/64459.

Hassane, A.I., Didane, D.H., Tahir, A.M., Mouangue, R.M., Tamba, J.G., Hauglustaine, J.-M., (2022). Comparative Analysis of Hybrid Renewable Energy Systems for Off-Grid Applications in Chad. *Int. J. Renew. Energy Dev.* 11(1), 49-62. https://doi.org/10.14710/ijred.2022.39012.

Heffel, J.W., (2003). NOx emission and performance data for a hydrogen fueled internal combustion engine at 1500rpm using exhaust gas recirculation. *Int. J. Hydrogen Energy* 28, 901–908. https://doi.org/10.1016/S0360-3199(02)00157-X.

Hoang, A.T., (2021). Combustion behavior, performance and emission characteristics of diesel engine fuelled with biodiesel containing cerium oxide nanoparticles: A review. *Fuel Process. Technol.* 218, 106840. https://doi.org/10.1016/j.fuproc.2021.106840.

Hoang, A.T., (2020a). Applicability of fuel injection techniques for modern diesel engines, in: *1st International Conference on Sustainable Manufacturing, Materials and Technologies. Coimbatore, India,* p. 020018. https://doi.org/10.1063/5.0000133.

Hoang, A.T., (2020b). Critical review on the characteristics of performance, combustion and emissions of PCCI engine controlled by early injection strategy based on narrow-angle direct injection (NADI). *Energy Sources, Part A Recover. Util. Environ. Eff.* 1–15. https://doi.org/10.1080/15567036.2020.1805048.

Hoang, A.T., Pham, V.V., (2020). A study on a solution to reduce emissions by using hydrogen as an alternative fuel for a diesel engine integrated exhaust gas recirculation. *AIP Conference Proceedings* 2235, 020035. https://doi.org/10.1063/5.0007492.

Hoang, A.T., Pham, V.V., (2021). 2-Methylfuran (MF) as a potential biofuel: A thorough review on the production pathway from biomass, combustion progress, and application in engines. *Renew. Sustain. Energy Rev.* 148, 111265. https://doi.org/10.1016/j.rser.2021.111265.

Huang, Z., Pandey, A., Luque, R., Ong, H.C., (2022). Characteristics of hydrogen production from steam gasification of plant-originated lignocellulosic biomass and its prospects in Vietnam. *Int. J. Hydrogen Energy* 47, 4394–4425. https://doi.org/10.1016/j.ijhydene.2021.11.091.

T.X. Nguyen-Thi and T.M.T. Bui *Int. J. Renew. Energy Dev 2023, 12(1), 118-128*

| 127

Huynh, T.T., Nguyen, X.P., Nguyen, T.K.T., Le, T.H., (2021). An analysis and review on the global NO$_2$ emission during lockdowns in COVID-19 period. *Energy Sources, Part A Recover. Util. Environ. Eff*. https://doi.org/10.1080/15567036.2021.1902431.

Imanuella, N., Witoon, T., Cheng, Y.W., Chong, C.C., Ng, K.H., Gunamantha, I., Lai, Y., (2022). Interfacial-engineered CoTiO$_3$-based composite for photocatalytic applications: a review. *Environ. Chem. Lett* 20, 3039–3069. https://doi.org/10.1007/s10311-022-01472-3.

Ji, C., Wang, S., (2011). Effect of hydrogen addition on lean burn performance of a spark-ignited gasoline engine at 800 rpm and low loads. *Fuel* 90, 1301–1304. https://doi.org/10.1016/j.fuel.2010.11.014.

Khandal, S. V, Banapurmath, N.R., Gaitonde, V.N., Hiremath, S.S., (2017). Paradigm shift from mechanical direct injection diesel engines to advanced injection strategies of diesel homogeneous charge compression ignition (HCCI) engines-A comprehensive review. *Renew. Sustain. Energy Rev*. 70, 369–384. https://doi.org/10.1016/j.rser.2016.11.058.

Konde, S.L., Yarasu, R.B., (2014). CFD Simulation and Geometrical Optimization of Producer Gas Carburetor. *IJETT* 13 (2), 59–62. https://doi.org/10.14445/22315381/IJETT-V13P212.

Lawrence, K.R., Balasubramanian, D., Gangula, V.R., Doddipalli, R.R., Bharathy, S., (2022). Exploration over combined impacts of modified piston bowl geometry and tert-butyl hydroquinone additive-included biodiesel/diesel blend on diesel engine behaviors. *Fuel* 322, 124206. https://doi.org/10.1016/j.fuel.2022.124206.

Le, A.T., Tran, D.Q., Tran, T.T., (2020). Performance and combustion characteristics of a retrofitted CNG engine under various piston-top shapes and compression ratios. *Energy Sources, Part A Recover. Util. Environ. Eff*. 1–17. https://doi.org/10.1080/15567036.2020.1804016.

Le, V.V., Nižetić, S., Tuan Le, A., Bui, V.G., (2021). Combustion and emission characteristics of spark and compression ignition engine fueled with 2,5-dimethylfuran (DMF): A comprehensive review. *Fuel* 288, 119757. https://doi.org/10.1016/j.fuel.2020.119757.

Lee, K.-T., Tsai, J.-Y., Gunarathne, D.S., Selvarajoo, A., Goodarzi, V., (2022). Energy-saving drying strategy of spent coffee grounds for co-firing fuel by adding biochar for carbon sequestration to approach net zero. *Fuel* 326, 124984. https://doi.org/10.1016/j.fuel.2022.124984.

Liu, X., Liu, F., Zhou, L., Sun, B., Schock, H.J., (2008). Backfire prediction in a manifold injection hydrogen internal combustion engine. *Int. J. Hydrogen Energy* 33, 3847–3855. https://doi.org/10.1016/j.ijhydene.2008.04.051.

Ma, F., Wang, Y., Liu, H., Li, Y., Wang, J., Zhao, S., (2007). Experimental study on thermal efficiency and emission characteristics of a lean burn hydrogen enriched natural gas engine. *Int. J. Hydrogen Energy* 32, 5067–5075. https://doi.org/10.1016/j.ijhydene.2007.07.048.

Malla, F.A., Mushtaq, A., Bandh, S.A., Qayoom, I., (2022). Understanding Climate Change: Scientific Opinion and Public Perspective, In: Bandh, S.A. (eds) *Climate Change. Springer, Cham*. https://doi.org/10.1007/978-3-030-86290-9_1.

Masson-Delmotte, V., Zhai, P., Pörtner, H.O., Roberts, D., Skea, J., Shukla, P.R., Pirani, A., Moufouma-Okia, W., Péan, C., Pidcock, R., (2018). Global warming of 1.5° C. *Intergovernmental Panel on Climate Change*. https://www.ipcc.ch/sr15/.

Nachippan, N.M., Parthasarathy, M., Elumalaib, P., Backiyaraj, A., Balasubramanian, D., (2022). Experimental assessment on characteristics of premixed charge compression ignition engine fueled with multi-walled carbon nanotube-included Tamanu methyl ester. *Fuel* 323, 124415. https://doi.org/10.1016/j.fuel.2022.124415.

Nayak, B., Singh, T.J., (2021). Experimental analysis of performance and emission of a turbocharged diesel engine operated in dual-fuel mode fueled with bamboo leaf-generated gaseous and waste palm oil biodiesel/diesel fuel blends. *Energy Sources, Part A Recover. Util. Environ. Eff*. 1–19. https://doi.org/10.1080/15567036.2021.2009595.

Nayak, S.K., Huang, Z., Ölçer, A.I., Wattanavichien, K., (2021). Influence of injection timing on performance and combustion characteristics of compression ignition engine working on quaternary blends of diesel fuel, mixed biodiesel, and t-butyl peroxide. *J. Clean. Prod*. 333, 130160. https://doi.org/10.1016/j.jclepro.2021.130160.

Nguyen, D.C., Hadiyanto, H., Wattanavichien, K., (2020). A Review on the Performance, Combustion, and Emission Characteristics of Spark-Ignition Engine Fueled With 2,5-Dimethylfuran Compared to Ethanol and Gasoline. *J. Energy Resour. Technol*. 143. https://doi.org/10.1115/1.4048228.

Nguyen, H.P., Nizetic, S., Nguyen, X.P., Le, A.T., Luong, C.N., Chu, V.D., (2021). The electric propulsion system as a green solution for management strategy of CO$_2$ emission in ocean shipping: A comprehensive review. *Int. Trans. Electr. Energy Syst*. 31, e12580. https://doi.org/10.1002/2050-7038.12580.

Nguyen, H.P., Le, A.T., Pham, V.V., Tran, V.N., (2020). Learned experiences from the policy and roadmap of advanced countries for the strategic orientation to electric vehicles: A case study in Vietnam. *Energy Sources, Part A Recover. Util. Environ. Eff*. 1–10. https://doi.org/10.1080/15567036.2020.1811432.

Nguyen, X.P., Ölçer, A.I., Huynh, T.T., (2021a). Record decline in global CO$_2$ emissions prompted by COVID-19 pandemic and its implications on future climate change policies. *Energy Sources, Part A Recover. Util. Environ. Eff*. 1–4. https://doi.org/10.1080/15567036.2021.1879969.

Nguyen, X.P., Le, N.D., Pham, V.V., Huynh, T.T., Dong, V.H., (2021b). Mission, challenges, and prospects of renewable energy development in Vietnam. *Energy Sources, Part A Recover. Util. Environ. Eff*. 1–13. https://doi.org/10.1080/15567036.2021.1965264.

Nižetić, S., Jurčević, M., Čoko, D., Arıcı, M., (2021). Implementation of phase change materials for thermal regulation of photovoltaic thermal systems: Comprehensive analysis of design approaches. *Energy* 228, 120546. https://doi.org/10.1016/j.energy.2021.120546.

Oladeji, A.S., Akorede, M.F., Aliyu, S., Mohammed, A.A., Salami, A.W., (2021). Simulation-Based Optimization of Hybrid Renewable Energy System for Off-grid Rural Electrification. *Int. J. Renew. Energy Dev*. 10(4), 667-686. https://doi.org/10.14710/ijred.2021.31316.

Ölçer, A., Le, V.V., Huynh, T.T., Le, A.T., Nayak, S.K., Pham, V.V., (2020). A remarkable review of the effect of lockdowns during COVID-19 pandemic on global PM emissions. *Energy Sources, Part A Recover. Util. Environ. Eff*. 1–16. https://doi.org/10.1080/15567036.2020.1853854.

Pandey, A., Huang, Z., Luque, R., Ng, Kim Hoong Papadopoulos, A., Chen, W.-H., Rajamohan, S., Hadiyanto, H., (2022). Catalyst-based synthesis of 2,5-dimethylfuran from carbohydrates as sustainable biofuel production route. *ACS Sustain. Chem. Eng*. 10(10), 3079–3115. https://doi.org/10.1021/acssuschemeng.1c06363.

Petar, V., Sandro, N., Ranjna, S., Ashok, P., Rafael, L., Kim, H.N., (2022). Perspective review on the municipal solid waste-to-energy route: Characteristics, management strategy, and role in the circular economy. *J. Clean. Prod*. 359, 131897. https://doi.org/10.1016/j.jclepro.2022.131897.

Pham, V.V., Hoang, A.T., (2019). Technological Perspective for Reducing Emissions from Marine Engines. *Int. J. Adv. Sci. Eng. Inf. Technol*. 9, 1989. https://doi.org/10.18517/ijaseit.9.6.10429.

Rajamohan, S., Gopal, A.H., Muralidharan, K.R., Huang, Z., Paramasivam, B., Ayyasamy, T., (2022). Evaluation of oxidation stability and engine behaviors operated by Prosopis juliflora biodiesel/diesel fuel blends with presence of synthetic antioxidant. *Sustain. Energy Technol. Assessments* 52, 102086. https://doi.org/10.1016/j.seta.2022.102086.

Rakopoulos, C.D., Michos, C.N., (2008). Development and validation of a multi-zone combustion model for performance and nitric oxide formation in syngas fueled spark ignition engine. *Energy Convers. Manag*. 49, 2924–2938. https://doi.org/10.1016/j.enconman.2008.02.011.

Rogelj, J., Geden, O., Cowie, A., Reisinger, A., (2021). Net-zero emissions targets are vague: three ways to fix. *Nature* 591, 365–368. https://doi.org/10.1038/d41586-021-00662-3.

Said, Z., Sharma, P., Tiwari, A.K., Huang, Z., (2022). Application of novel framework based on ensemble boosted regression trees and

T.X. Nguyen-Thi and T.M.T. Bui

Int. J. Renew. Energy Dev 2023, 12(1), 118-128

| 128

Gaussian process regression in modelling thermal performance of small-scale Organic Rankine Cycle (ORC) using hybrid nanofluid. *J. Clean. Prod.* 360, 132194. https://doi.org/10.1016/j.jclepro.2022.132194.

Sandro, N., Van, P.V., Anh, H.T., (2021). A state-of-the-art review on emission characteristics of SI and CI engines fueled with 2,5-dimethylfuran biofuel. *Environ. Sci. Pollut. Res.* 28, 4918–4950. https://doi.org/10.1007/s11356-020-11629-8.

Sharma, P., Sahoo, B.B., Said, Z., Hadiyanto, H., Huang, Z., Li, C., (2022a). Application of machine learning and Box-Behnken design in optimizing engine characteristics operated with a dual-fuel mode of algal biodiesel and waste-derived biogas. *Int. J. Hydrogen Energy.* https://doi.org/10.1016/J.IJHYDENE.2022.04.152.

Sharma, P., Kumar, A., Pandey, A., Afzal, A., Li, C., (2022b). Recent advances in machine learning research for nanofluid-based heat transfer in renewable energy system. *Energy & Fuels* 36, 6626–6658. https://doi.org/10.1021/acs.energyfuels.2c01006.

Sharma, P., Said, Z., Memon, S., Elavarasan, R.M., Khalid, M., Arıcı, M., (2022c). Comparative evaluation of AI-based intelligent GEP and ANFIS models in prediction of thermophysical properties of Fe_3O_4-coated MWCNT hybrid nanofluids for potential application in energy systems. *Int. J. Energy Res.* 46(13), 19242-19257. https://doi.org/10.1002/er.8010.

Subramanian, K.A., Salvi, B.L., (2016). A numerical simulation of analysis of backfiring phenomena in a hydrogen-fueled spark ignition engine. *J. Eng. Gas Turbines Power* 138. https://doi.org/10.1115/1.4033182.

Subramanian, M., Kalidasan, B., Soloman, J.M., Balasubramanian, D., Subramaniyan, C., Thenmozhi, G., Metghalchi, H., (2021). A technical review on composite phase change material based secondary assisted battery thermal management system for electric vehicles. *J. Clean. Prod.* 322, 129079. https://doi.org/10.1016/j.jclepro.2021.129079.

Tabatabaei, M., Aghbashlo, M., Carlucci, A.P., Ghassemi, A., (2021). Rice bran oil-based biodiesel as a promising renewable fuel alternative to petrodiesel: A review. *Renew. Sustain. Energy Rev.* 135, 110204. https://doi.org/10.1016/j.rser.2020.110204.

Tran, V.D., Dong, V.H., Le, A.T., (2022). An experimental analysis on physical properties and spray characteristics of an ultrasound-assisted emulsion of ultra-low-sulphur diesel and Jatropha-based biodiesel. *J. Mar. Eng. Technol.* 21, 73–81. https://doi.org/10.1080/20464177.2019.1595355.

Vakili, S., Ölçer, A.I., Schönborn, A., Ballini, F., (2022). Energy-related clean and green framework for shipbuilding community towards zero-emissions: A strategic analysis from concept to case study. *Int. J. Energy Res.* 46(14), 20624-20649. https://doi.org/10.1002/er.7649.

Vali, R.H., Wani, M.M., Pali, H.S., Balasubramanian, D., Arıcı, M., (2022). Optimization of variable compression ratio diesel engine fueled with Zinc oxide nanoparticles and biodiesel emulsion using response surface methodology. *Fuel* 323, 124290. https://doi.org/10.1016/j.fuel.2022.124290.

Veza, I., Afzal, A., Mujtaba, M.A., Balasubramanian, D., Sekar, M., Fattah, I.M.R., Soudagar, M.E.M., EL-Seesy, A.I., Djamari, D.W., (2022a). Review of artificial neural networks for gasoline, diesel and homogeneous charge compression ignition engine. *Alexandria Eng. J.* 61, 8363–8391. https://doi.org/10.1016/j.aej.2022.01.072.

Veza, I., Karaoglan, A.D., Ileri, E., Afzal, A., Tamaldin, N., Herawan, S.G., Abbas, M.M., Said, M.F.M., (2022b). Multi-objective optimization of diesel engine performance and emission using grasshopper optimization algorithm. *Fuel* 323, 124303. https://doi.org/10.1016/j.fuel.2022.124303.

Veza, I., Karaoglan, A.D., Ileri, E., Kaulani, S.A., Tamaldin, N., Latiff, Z.A., Said, M.F.M., Yatish, K. V, Idris, M., (2022c). Grasshopper optimization algorithm for diesel engine fuelled with ethanol-biodiesel-diesel blends. *Case Stud. Therm. Eng.* 31, 101817. https://doi.org/10.1016/j.csite.2022.101817.

Veza, I., Said, M.F.M., Latiff, Z.A., (2021). Recent advances in butanol production by acetone-butanol-ethanol (ABE) fermentation. *Biomass and Bioenergy* 144, 105919. https://doi.org/10.1016/j.biombioe.2020.105919.

Vinayagam, N.K., Solomon, J.M., Subramaniam, M., Balasubramanian, D., EL-Seesy, A.I., (2021). Smart control strategy for effective Hydrocarbon and Carbon monoxide emission reduction on a conventional diesel engine using the pooled impact of pre-and post-combustion techniques. *J. Clean. Prod.* 306, 127310. https://doi.org/10.1016/j.jclepro.2021.127310.

Wang, J.-S., Chang, M.-H., Lam, S.S., Kwon, E.E., Ashokkumar, V., (2022). Optimization of a vertical axis wind turbine with a deflector under unsteady wind conditions via Taguchi and neural network applications. *Energy Convers. Manag.* 254, 115209. https://doi.org/10.1016/j.enconman.2022.115209.

Xuan, N.P., Van, P.V., Anh, H.T., (2021). Integrating renewable sources into energy system for smart city as a sagacious strategy towards clean and sustainable process. *J. Clean. Prod.* 305, 127161. https://doi.org/10.1016/j.jclepro.2021.127161.